ACS Chemical Neuroscience

Research Article

pubs.acs.org/chemneuro

Amperometric Detection of Single Vesicle Acetylcholine Release Events from an Artificial Cell

Jacqueline D. Keighron,[†] Joakim Wigström,[†] Michael E. Kurczy,[†] Jenny Bergman,[‡] Yuanmo Wang,[†] and Ann-Sofie Cans*,[†]

[†]Department of Chemical and Biological Engineering, Chalmers University of Technology, 41296 Gothenburg, Sweden

[‡]Department of Chemistry and Molecular Biology, University of Gothenburg, 41296 Gothenburg, Sweden

Supporting Information

ABSTRACT: Acetylcholine is a highly abundant nonelectroactive neurotransmitter in the mammalian central nervous system. Neurochemical release occurs on the millisecond time scale, requiring a fast, sensitive sensor such as an enzymatic amperometric electrode. Typically, the enzyme used for enzymatic electrochemical sensors is applied in excess to maximize signal. Here, in addition to sensitivity, we have also sought to maximize temporal resolution, by designing a sensor that is sensitive enough to work at near monolayer enzyme coverage. Reducing the enzyme layer thickness increases sensor temporal resolution by decreasing the distance and reducing the diffusion time for the enzyme product to travel to the sensor surface for detection. In this instance, the sensor consists of electrodeposited gold nanoparticle modified carbon fiber microelectrodes (CFMEs). Enzymes often are sensitive to curvature upon surface adsorption; thus, it was important to deposit discrete nanoparticles to maintain enzyme activity while depositing as much gold as possible to maximize enzyme coverage. To further enhance sensitivity, the enzymes acetylcholinesterase (AChE) and choline oxidase (ChO) were immobilized onto the gold nanoparticles at the previously determined optimal ratio (1:10 AChE/ChO) for most efficient sequential enzymatic activity. This optimization approach has enabled the rapid detection to temporally resolve single vesicle acetylcholine release from an artificial cell. The sensor described is a significant advancement in that it allows for the recording of acetylcholine release on the order of the time scale for neurochemical release in secretory cells.

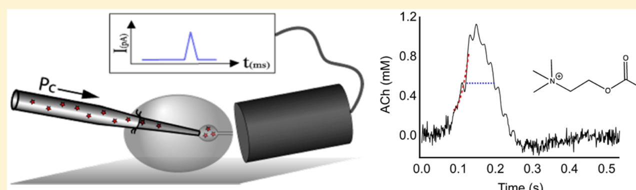

KEYWORDS: *Biosensor, acetylcholine, artificial cell, exocytosis, amperometry, gold nanoparticles, enzymes*

Acetylcholine (ACh) is a neurotransmitter that is involved in communication in both the central and peripheral mammalian nervous systems. In the central nervous system, it participates in a range of functions including reward, learning and memory, mood, sensory processing, pain, and neuroprotection.[1−4] Increasing our knowledge of how ACh participates in these processes is important, for instance, for a better understanding of the pathways where ACh is involved and in explaining the effects of pharmacological substances in the development of new drugs.

A range of analytical techniques exists for investigating the role of the cholinergic pathways. In vivo microdialysis, due to its sensitivity and specificity in detection, stands out as one of the most important techniques for probing the chemical microenvironment of the brain.[5] Placement of the microdialysis probe and sampling of extracellular fluid in the brain has made it possible to study the relationship between complex cognitive behavior and cholinergic activation.[5,6] One weakness of conventional microdialysis is the temporal resolution where an optimal resolution would be able to record dynamics of acetylcholine behavior on a subsecond time scale. Microdialysis sampling times on the time scale of several minutes are often required to collect sufficient amounts of analyte for ACh detection.[5] Although advances in detection have successively reduced the length of collection times by fractionation of microdialysis fluid into water-in-oil droplets, sampling times down to 5 s have been achieved.[7] Additionally, the spatial resolution for microdialysis is difficult to estimate and may extend several millimeters from the dialysis probe,[8,9] which can extend beyond specific brain regions and certainly far beyond the dimensions of a single cell. These limitations make it difficult to relate ACh activity to specific animal behavioral responses[6,10] or to separate cholinergic activation in adjacent brain regions.

In situ electrochemical detection techniques offer dramatically improved temporal and spatial resolution compared to microdialysis.[2,15] Direct positioning of electrodes in brain tissue has been applied to in vivo studies of release and uptake of electroactive neurotransmitters such as epinephrine, norepinephrine, dopamine, and serotonin.[11] In situ carbon fiber or platinum wire electrodes are orders of magnitude smaller, compared to microdialysis tubes, with diameters often seen in

Special Issue: Monitoring Molecules in Neuroscience 2014

Received: October 23, 2014
Revised: January 6, 2015
Published: January 7, 2015

© 2015 American Chemical Society

DOI: 10.1021/cn5002667
ACS Chem. Neurosci. 2015, 6, 181−188

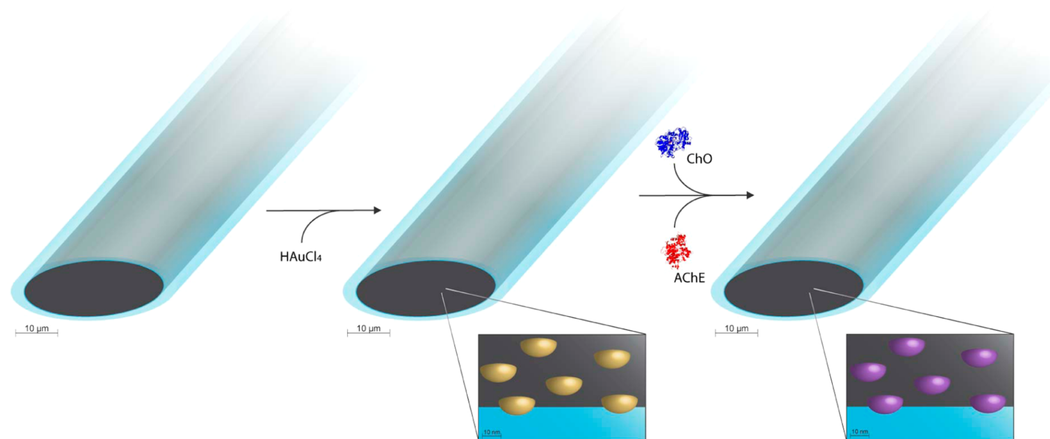

Figure 1. Electrode functionalization. Discrete gold nanoparticles were deposited onto the surface of a 30 μm disk electrodes from a solution of $HAuCl_4$. AChE and ChO were then immobilized onto the functionalized electrode to create the final biosensor design.

the range of 5−30 μm. The comparatively small probe size allows for micrometer scale spatial resolution.[9] Since detection of neurochemical release occurs directly at the electrode surface, extracellular neurotransmitter concentration can be measured at subsecond time scales.[9,12]

Carbon fiber microdisk electrodes have provided a useful tool for fundamental studies of secretion of electroactive neurotransmitters from single cells in cell culture.[11,13] When placed adjacent to the surface of the studied cell, these electrodes achieve a time resolution sufficient to resolve kinetic parameters of the neurotransmitter release from individual exocytotic vesicles. Such single-cell experiments have provided fundamental knowledge on the mechanisms of neurotransmitter release, the regulation by exocytotic proteins, and the effects of drug on quantal size and fusion pore dynamics.[11,13,14]

To allow in vivo detection of electroinactive analytes, enzyme based microelectrodes have been developed.[12,15] At these sensor surfaces, nonelectroactive analytes are catalyzed by immobilized enzymes, producing an electroactive reporter molecule, such as hydrogen peroxide, that can be detected electrochemically. As a further development of this technique, to enhance selectivity in the measurements, microelectrode arrays has been developed consisting of separate electrodes with different surface functionalities for detection of interfering compounds,[10,15−17] allowing a self-referencing technique. Although these sensors have reported a high sensitivity and selectivity, the enzyme based sensors have been limited by a second to subsecond time resolution in the detection of nonelectroactive neurotransmitters such as ACh, which is still not fast enough for monitoring individual exocytosis events.

Most electrochemical enzyme-based biosensors consist of an electrode surface, covered with large amounts of enzyme material to convert a nonelectroactive species into an electroactive product. In this work, we further our previous efforts of characterizing the interactions of acetylcholinesterase (AChE) and choline oxidase (ChO) with gold nanoparticles (AuNP)[18,19] in order to improve on existing acetylcholine biosensors. Here we describe the characterization and optimization of discrete nanoparticles on the surface of a 30 μm electrode to create a nanostructured surface suitable for monolayer enzyme deposition of AChE and ChO, as illustrated by the schematics on the sensor construction in Figure 1. Finally, we have used this sensor to monitor exocytosis of ACh from an artificial secretory cell to highlight the temporal capabilities of the sensor.[26]

■ RESULTS AND DISCUSSION

Characterization of Functionalized CFME Surface. *AuNP Deposition.* Carbon fiber microelectrodes (CFME; 30 μm) were functionalized with AuNP by electrodeposition of $HAuCl_4$ in 0.5 M sulfuric acid. Briefly, disk electrodes, beveled at 45°, were placed in a solution of 0.3 mM or 0.5 mM $HAuCl_4$ with a Ag/AgCl reference electrode. Reduction of Au^{3+} to Au^0 was achieved by applying a constant potential of −0.6 V for 2−32 s. As seen in Figure 2A and B, this resulted in the formation of discrete AuNP across the carbon surface of the electrode.

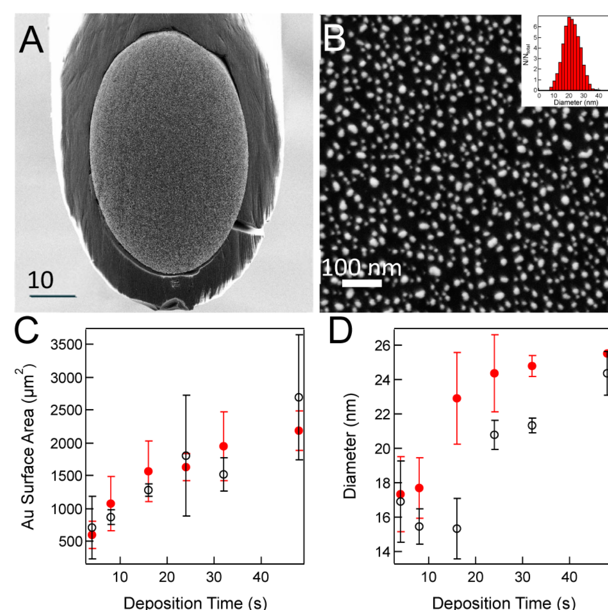

Figure 2. Characterization of nanoparticle functionalized electrodes. (A) SEM image of the tip of a 30 μm functionalized electrode. (B) Representative image of the deposited nanoparticles; inset histogram of the nanoparticle diameter. (C) Relationship between deposition time and the gold surface area measured by linear sweep voltammetry. (D) Relationship between deposition time and the diameter of deposited nanoparticles. Open symbols, 0.3 mM $HAuCl_4$; filled red symbols, 0.5 mM $HAuCl_4$.

DOI: 10.1021/cn5002667
ACS Chem. Neurosci. 2015, 6, 181−188

This arrangement was found optimal to (a) provide a gold surface that was 100% accessible for enzyme modification, (b) maintain the flat electrode geometry necessary for single cell amperometry, and (c) leave an open carbon surface, making the electrode capable of multianalyte detection.

The deposition time and $HAuCl_4$ concentration were optimized by determining the average diameter of the deposited AuNP, through scanning electron microscopy (SEM), as well as the total Au surface area present on the electrode, through linear voltammetry. The average deposited AuNP surface area is shown in Figure 2C as a function of deposition time. As expected, longer deposition times result in a greater amount of AuNP being deposited on the electrode surface, but the concentration of $HAuCl_4$ in solution did not appear to have a significant effect on the amount of gold deposited. Figure 2D illustrates the effect of deposition time on the diameter of electrodeposited AuNP with both 0.3 and 0.5 mM $HAuCl_4$. Here, the $HAuCl_4$ concentration did appear to have an effect on the diameter of the AuNPs, with higher concentrations producing fewer, larger nanoparticles with less deposition time.

In the design of this biosensor, the curvature of the AuNPs is of great interest. Previous work has shown that when enzymes are adsorbed onto relatively flat surfaces, a large portion of their tertiary structure is changed, resulting in significant losses of activity.[27] However, when enzymes are adsorbed onto a highly curved surface, they retain more of their native structure and function. For the next steps of this work, a AuNP diameter around 20 nm was desired, so a deposition time of 24 s in a solution of 0.5 mM $HAuCl_4$ was selected.

Enzyme Deposition. The sequential chain of reactions from the analyte, ACh, leading to detection of hydrogen peroxide is shown below. First, ACh is hydrolyzed by AChE, forming acetate and choline, reaction 1. Thereafter, choline can be oxidized by ChO forming hydrogen peroxide and betaine aldehyde, reaction 2, which is further oxidized, forming one additional hydrogen peroxide and betaine, reaction 3. Finally, hydrogen peroxide is reduced at the electrode, reaction 4.

$$\text{acetylcholine} + H_2O \rightarrow \text{acetate} + \text{choline} \quad (1)$$

$$\text{choline} + O_2 \rightarrow \text{betaine aldehyde} + H_2O_2 \quad (2)$$

$$\text{betaine aldehyde} + O_2 + H_2O \rightarrow \text{betaine} + H_2O_2 \quad (3)$$

$$H_2O_2 + 2H^+ + 2e^- \rightarrow H_2O \quad (4)$$

To achieve selectivity in detection from the majority of potential interfering agents, that can be oxidized, electrochemical reduction of hydrogen peroxide was chosen as the method for detection. Several previous reports have demonstrated the advantages of single layer enzyme coverage in nanoparticle bioconjugates.[24,25] The absence of excess material allows for (a) greater accessibility of the enzyme active site, (b) reduced chance for steric hindrances to enzyme activity, and (c) faster diffusion of the enzymatic product to the electrode surface.

In our previous work, we used analytical methods to quantify the number of AChE and ChO bound to the surface of 14 nm gold nanoparticle colloids to characterize the enzyme/gold nanoparticle conjugate stoichiometry and activity for the detection of acetylcholine.[19] This was evaluated by the retained enzymatic efficiency of AChE and ChO after the enzyme/gold nanoparticle synthesis.[19] Following the results from this previous work, showing optimum conditions of depositing AChE:ChO at the ratio of 1:10 from solution onto the gold nanoparticles in bulk, we immobilized AChE and ChO at a 1:10 ratio from solution onto the electrodeposited gold nanoparticles of the sensor surface in this work. The AuNP modified electrodes were functionalized with enzymes from a dilute solution (0.22 mg/mL total enzyme content) for a relatively short period of time, 90 min at room temperature or overnight at 4 °C. This procedure allowed for a minimal amount of enzyme to be adsorbed and cover the electrode surface, creating the advantages noted above.

To characterize the enzymes adsorbed to the biosensor surface, fluorescent and enzymatic assays were used. Briefly, prior to adsorption onto the AuNP modified electrode, AChE and ChO were fluorescently labeled with Alexa Fluor 488 and Alexa Fluor 555, respectively. After the enzymes were deposited on the electrode surface, the biosensor was washed with water, allowed to dry, and then placed in a solution of potassium cyanide (pH 8) to dissolve the AuNP and release the enzymes into solution. The amount of each enzyme present on the electrode surface was then measured fluorescently and correlated to the AuNP surface area measured by linear voltammetry. These results (Table 1) indicate that AChE and ChO deposited in a roughly 1:2 ratio, with similar coverage rates to what was previously reported for each enzyme to AuNP in bulk solution, 1.3×10^5 μm^{-2} AChE and 9.2×10^5 μm^{-2} ChO.[6] For this estimate, only enzymes attached to gold are assumed to be removed by the cyanide treatment. The greater coverage in this case could be due to the slightly different curvature of the AuNP surface, 20 nm on the electrode and 14 nm in solution.

Table 1. Characterization of Immobilized Enzymes

	AChE	ChO
surface coverage (enzyme/μm^2)	$7.4 \times 10^5 \pm 16\%$	$1.5 \times 10^6 \pm 6\%$
activity (U/μm^2)	$1.84 \times 10^{-11} \pm 43\%$	$1.19 \times 10^{-11} \pm 48\%$
specific activity (immobilized) (mU/mg)	224 ± 96	73 ± 35
specific activity (free enzyme)[19] (U/mg)	1000	10
detection rate (μmol/ms)	0.43 ± 0.18	0.28 ± 0.13

Along with enzymatic assays, the enzyme coverage information was used to characterize the retained activity of each immobilized enzyme (Table 1). In the reaction used here, the analyte of interest, acetylcholine, is converted to choline by AChE. Choline is then catalyzed to H_2O_2 by ChO, which can be consumed at the electrode surface.[20] The activity/μm^2 shows how catalytically active the biosensor is to both acetylcholine and choline. On average, the sensor is capable of catalyzing more acetylcholine than choline; this may limit the efficiency of the detection of acetylcholine at high concentrations.

As demonstrated in our previous work,[19] the extent of the activity mismatch between AChE and ChO makes it difficult to achieve a setup where the enzymatic process could be 100% efficient. Therefore, only by carefully characterizing the immobilized enzymes and determining the optimal ratio of AChE and ChO to the AuNP at the conjugation process, we have been able to minimize the impact of the mismatch on the overall detection of acetylcholine.

DOI: 10.1021/cn5002667
ACS Chem. Neurosci. 2015, 6, 181−188

The specific activity (Table 1) is a measure of how well each enzyme is working, and can be compared to the value found for the unmodified enzyme to determine the effect immobilization has had on enzyme activity and structure. Even though the enzymes have been placed onto a high curvature nanostructured material at the electrode surface, as compared to enzymes adsorbed to a flat surface, denaturation upon adsorption during the immobilization of both AChE and ChO still results in a significant loss of activity. This is likely due to changes in the tertiary structure of the enzymes or blockage of the active site by the orientation of enzyme at adsorption to the electrode surface.[24,25] However, if the sensor is considered as a whole, an overall detection rate can be calculated for ACh and choline. The detection rate is defined as the number of molecules of reactant detected per millisecond under saturating substrate conditions; by accounting for the U/μm^2 and the total area of AuNP present on the electrode, an overall rate can be calculated. As seen in Table 1, the sensor is capable of quickly processing both acetylcholine and choline.

Due to the relatively low concentrations of acetylcholine released during exocytosis (2000−20 000 molecules depending on species),[36] catalytic mismatch and loss of activity may not significantly limit the function of the biosensor since the detection rate of the sensor is high enough for this number. For this mismatch to affect the detection of the sensor, the rate of acetylcholine release would have to exceed the catalytic rate of ChO on the average electrode, that is, more than 140 000 molecules/ms. However, it is interesting to note that most enzyme-based biosensors are not characterized in this manner and, therefore, may not be optimized to for detection of vesicular release of acetylcholine.

Characterization of the Biosensor. *Biosensor Sensitivity.* In this biosensor design, the amount of AuNP deposited on the surface is strongly linked to the overall sensitivity. AuNPs perform two functions in this design: (1) to provide a scaffold for enzyme immobilization and (2) to provide a surface that is readably available for H_2O_2 reduction. Testing the response of H_2O_2 by a voltage scan from −0.75 to 0 V vs Ag/AgCl reference electrode at 0.1 V/s showed no response at a bare carbon microelectrode surface and a reduction current detected at the gold nanoparticle coated electrode surface, as shown in Supporting Information Figure S1. Hence, as shown in earlier literature, H_2O_2 is detected by the gold surface and not by the carbon surface at the potential used for acetylcholine sensing in these experiments.[20] Figure 3A shows the detection of 25 mM acetylcholine as a function of the AuNP surface area. As can be expected, the amount of signal generated increases with the increase in surface area as more total enzyme is present and there is more available surface for H_2O_2 to react. This relationship is not completely linear; when very high quantities of AuNP are deposited on the CFME surface, the signal no longer increases above a certain threshold. This may be due to the progressive loss of curvature as the coverage increases. Loss of curvature may affect activity of the enzymes as well adsorption. Furthermore, the change to a flat surface may reduce the surface area available to quickly reduce the H_2O_2 produced. Electrodes modified with 1200−1400 μm^2 of AuNP were therefore used to complete all further experiments, as they displayed a maximal detection rate without the presence of unusable surface area.

To account for the variability in the deposition of AuNPs for total AuNP, surface area was measured electrochemically for each sensor and used as a correction factor so that the output of multiple sensors could be compared. Figure 3B shows the calibration of the sensor to ACh. By using a wide range of concentrations, a Michaelis−Menten curve was generated revealing that the biosensor had a K_M value of 10 ± 2 mM. This value demonstrates the affinity of ACh for the enzymes on the biosensor surface. Typically, enzymes in solution have K_M values ranging between 10^{-1} M (low affinity) and 10^{-7} M (high affinity),[28] while the reported K_M value for ACh with AChE has been reported to be 0.0739 mM.[35] This indicates a significant loss in affinity for ACh once the enzymes have been immobilized, but may not limit the functionality of the sensor. This is still comparable to recently published results. Additionally, the K_M values often cited are for enzyme free in solution; the nature of this sensor dictates that both diffusion and charge transfer to the electrochemical system will also influence the measured K_M value, likely in an unfavorable way. In our previous characterization of AChE and ChO with AuNP, it has been demonstrated that the catalysis of ACh is enhanced when both enzymes are present.[19] Possible explanations for this are (1) catalysis of ACh by ChO[19] and (2) changes in the adsorption of AChE to AuNP by the presence of ChO, similar to the effects seen before with another enzyme pair, malate dehydrogenase and citrate synthase.[25]

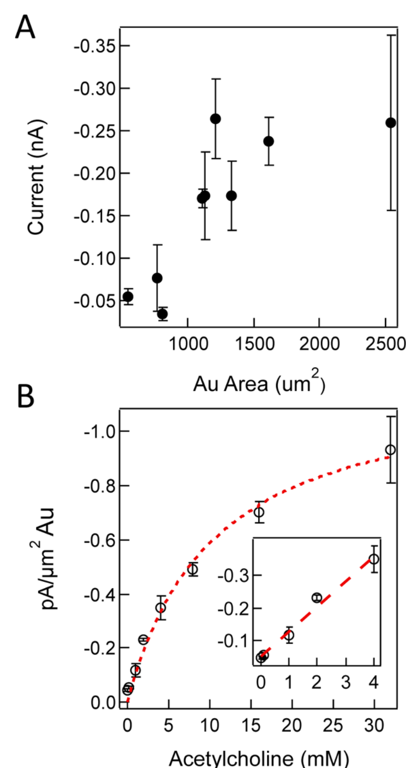

Figure 3. Electrode sensitivity. (A) The signal generated from exposure to 25 mM acetylcholine is related to the AuNP surface area of individual electrodes. $n = 5$, error shown as standard deviation. (B) By accounting for the AuNP surface area, a reproducible calibration was found, with K_M = 10 ± 2 mM. Inset: linear range of detection ranges from 10 μM to 4 mM with R^2 of 0.987. $n = 10−15$, error shown as standard error of the mean.

At lower concentrations of ACh, the biosensor does demonstrate a linear range covering 2 orders of magnitude in concentration, from 10 μM to 4 mM with an R^2 constant of 0.987, which is on par with other detection methods.[29−31] The sensor sensitivity determined by the sensor linear range of response was 0.07 pA per mM acetylcholine and per μm^2 Au

DOI: 10.1021/cn5002667
ACS Chem. Neurosci. 2015, 6, 181−188

surface area. The limit of detection for this sensor defined by the ACh concentration detected with 3 times the RMS value was 10 μM. This is similar sensitivity to other electrochemical methods for ACh detection and many of which have been reported between 0.08 and 11 μM.[10,29−31] For in vivo recordings, the expected range of ACh in rat brains is expected in the low micromolar range,[10] and perhaps at the limit for this sensor to resolve. In addition, even though this sensor has shown potential for higher temporal recordings of individual vesicle release events of ACh from an artificial cell model, the sensitivity needed, for example, to resolve individual 50 nm diameter ACh granules containing 100 mM ACh hence still remains a challenge.

Biosensor Selectivity. The specificity of the biosensor for the analyte of interest is of great importance for in vivo application. To determine what kind of interfering signals the sensor would detect, several biologically relevant substances were tested: the electroactive neurotransmitters dopamine and norepinephrine, the nonelectroactive neurotransmitter glutamate, and two commonly found biological molecules, ascorbic acid and glucose. At lower physiologically relevant concentrations (sub-μM to low μM), we were not able to detect these potentially interfering analytes. However, as seen in Figure 4, higher concentrations (5 mM) of each species did produce small responses at the sensor surface, though none of these responses were greater than 35% of the acetylcholine signal. Detection of some of these analytes may be due to nonspecific catalysis by choline oxidase, producing H_2O_2 at low rate from interfering molecules such as glucose and glutamate.[19,32,33] While the natively electroactive molecules may react with the carbon and gold surfaces at the low potential (−0.5 V) used in these experiments, in true biological samples the concentration of each of these analytes is far lower than the 5 mM needed for detection with this biosensor, suggesting that interfering species will not be a limitation for in vivo detection of ACh. The response to choline and ACh and the interference of H_2O_2 at gold nanoparticle coated electrodes was also characterized for electrodes coated with ChO, AChE, or with ChO together with AChE and show potential interference of H_2O_2 at higher concentrations (Supporting Information Figure S2).

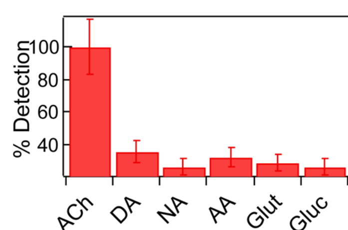

Figure 4. Selectivity of the biosensor. Electrodes were exposed to 5 mM acetylcholine solution and 5 mM solutions of possible interfering compounds in a flow system with potential set to −0.5 V. Signal is not calculated per AuNP area due to the possibility of interactions with the carbon surface.

Biosensor Stability. In the performance of repeated 15−20 injections of ACh solution over the time course of 4 h, there was no significant difference in sensor response. Additionally testing the sensors after usage and storage in the fridge at 4 °C, the response to 25 mM ACh was remeasured after 10 days and showed that 88 ± 15% activity remained (n = 3).

Time Resolved Detection of Acetylcholine. *Acetylcholine Detection in a Model System.* In many biological systems, neurotransmitters such as ACh are released as a chemical signal between neighboring nerve cells. While natively electroactive species such as dopamine, epinephrine, norepinephrine, and serotonin are readily detected with a CFME, nonelectroactive species such as acetylcholine are not.

In order to detect ACh as a neurotransmitter, a sensitive, selective biosensor with precise temporal resolution is necessary. In this work, we have employed a previously described[22] artificial cell model for exocytosis to evaluate our sensor for single cell analysis. Briefly, an artificial secretory cell was formed by first creating a lipid nanotube within a giant

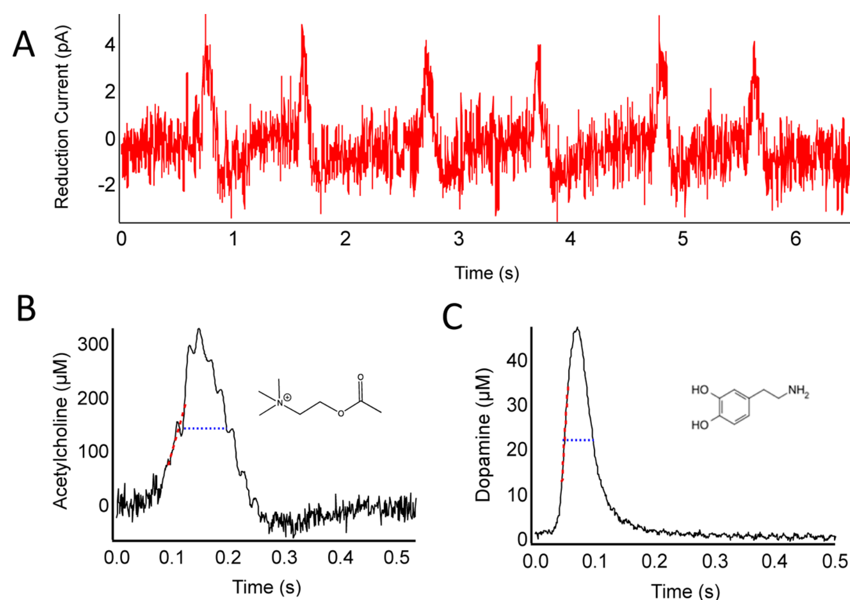

Figure 5. Time resolved detection of acetylcholine. (A) Representative trace of repeated exposure to acetylcholine from the artificial cell model. (B) The average spike (−0.4 V) from acetylcholine (12.5 mM) shows detection occurs in 10s of ms, while (C) the average spike (+0.8 V) with an electroactive molecule, dopamine, demonstrates detection on a similar time scale. The spikes presented in parts (B) and (C) are average spikes generated by averaging n > 10 individual events.

DOI: 10.1021/cn5002667
ACS Chem. Neurosci. 2015, 6, 181−188

unilamellar vesicle connecting the outer membrane to a glass micropipet. By inflating the nanotube with solution, an artificial exocytosis vesicle is formed which under constant pressure will repeatedly grow until it fuses with the outer membrane.

Figure 5A shows an example of an amperometric trace from the reduction of H_2O_2 produced by ACh catalysis on the biosensor surface from individual vesicle release events. Since the content of each event is controlled by the model system, each corresponding amperometric signal has reproducible peak amplitude or I_{max} (±7.7%) and event time or $t_{1/2}$ (±2.3%) over the course of 30 or more individual events.

Comparison to Dopamine Detection. To evaluate how the enzyme functionalized biosensor detects events, it was compared to a natively active neurotransmitter, dopamine, on the same biosensor surface. This was possible because the sensor contains both AuNP and bare carbon surfaces, allowing for the enhanced reduction of H_2O_2 on the gold surface, while dopamine can be oxidized easily on the carbon surface. Figure 5B and C shows the average spike associated with acetylcholine and dopamine detection, respectively.

Time specific parameters relating to the detection of acetylcholine in each independent event can be measured from the corresponding amperometric spike. Specifically, the duration of the event ($t_{1/2}$) can be estimated from the full with at half-maximum of the event, the response time can be determined from the 25−75% initial rise time of the event (t_{rise}), and the clearance of acetylcholine from the biosensor surface (t_{fall}) can be found in the decay following the maximum peak height. A list of these pooled parameters can be found in Table 2.

Table 2. Characterization of Artificial Exocytosis

	acetylcholine	dopamine
$t_{1/2}$ (ms)	79 ± 2	46.3 ± 0.4
t_{rise} (ms)	39 ± 6	15.9 ± 0.3
t_{fall} (ms)	54 ± 3	23.8 ± 0.7

Response Time. As is evident from Figure 5B and Table 2, each event from beginning to end occurs in less than 100 ms. The rise time of the current spike, t_{rise}, is on average 40 ms, which corresponds to the detection of ACh release from a vesicle fusion pore opening and dilation and content release. This recording of vesicle ACh release from this model cell for exocytosis is very fast in comparison to some recently reported methods for acetylcholine detection using carbon nanotubes (5 s),[29] conductive polymers (7 s),[34] or L_BL entrapment,[31] although faster detection of acetylcholine has been detected in vivo on the second to subsecond time scale.[10] We hypothesize this increase in time resolution is due to several factors. First, in our recently published study, the immobilization of enzymes on to the nanoparticulate gold surface was optimized to maximize H_2O_2 production.[19] Second, limiting the amount of material at the electrochemical surface may increase the rate of detection by increasing the rate of diffusion of analytes to enzymes, and products to the electrochemical surface, in contrast to the reported cases where excess material on the surface has proven to decrease sensitivity[30,31] or response time. Finally, the biological mimic test system employed in this experiment allowed for very small, rapid events to take place that maximized the introduction and clearance of analytes to and from the electrochemical surface.

In conclusion, we have in this work characterized an ACh sensor based on the interactions of AChE and ChO with electrodeposited AuNPs for the fast, sensitive detection of ACh released by exocytosis. In order to make a sensor with extremely fast time resolution, it was necessary to carefully consider several parameters: interactions of AChE and ChO with AuNPs, redox chemistry of H_2O_2, and carefully limiting the enzyme material thickness to a very thin layer covering the electrode surface.

In order to gauge the time resolution of the sensor, we employed a cell model for exocytosis, which allowed for precise application of small test quantities of vesicular ACh release to the electrode surface in a short time frame. Our results indicate that the detection of ACh release from the model cell for exocytosis occurs at nearly the same rate as dopamine, a natively electroactive species, and a fast sensor in comparison to other reported ACh sensors. This new approach in enzyme based electrochemical sensor design opens the possibility for detection of nonelectroactive neurotransmitter release to be detected on time scales needed for single vesicle release events at exocytosis and for applications of neurochemical recordings at single cells as well as for better sampling of temporal dynamic changes of these analytes in vivo in the brain.

■ METHODS

Materials. Alexa Fluor 488 and Alexa Fluor 555 protein labeling kits were purchased from Invitrogen (Carlsbad, CA). AChE from electric eel, ChO from *Alcaligenes* sp., acetylcholine chloride, choline chloride, hydrogen peroxide (30%), sodium phosphate dibasic, potassium phosphate monobasic, sodium chloride, potassium chloride, potassium cyanide, sodium bicarbonate, gallium, sulfuric acid, tetracloroaurate, ferrocene-methanol, and tungsten wire were purchased from Sigma-Aldrich (St. Louis, MO). Whatman 20 nm pore diameter syringe filters were purchased from VWR. Deionized water with resistivity ≥ 18 MΩ was used in all experiments.

Preparation of 33 μm CFME. Carbon fiber microelectrodes were prepared by aspirating single 33 μm diameter carbon fibers (Cytec Engineered Materials, Tempe, AZ) into borosilicate glass capillaries (1.2 mm OD, 0.69 mm ID, Sutter Instrument Co., Novato, CA). The filled capillaries were then pulled to a taper using a commercial micropipet puller (model PE-21, Narishige, Inc., London, U.K.), and epoxy (Epoxy Technology, Billerica, MA) was used to seal the glass-carbon fiber junction of the electrode. The electrode tips were cut using a scalpel and polished at a 45° angle on a diamond dust-embedded micropipet beveling wheel (Narishige, Inc., London, U.K.). Electrodes were tested in a 100 μM ferrocene/methanol solution before experiments, and only electrodes with stable *I*−*E* curves were used.

Functionalization with AuNP. Electrodes were functionalized with AuNP by an electrochemical deposition method similar to that of Finot et al.[21] with minor alterations. The CFME and a Ag/AgCl reference electrode were immersed in a 0.5 mM solution of $HAuCl_4$ in 0.5 M H_2SO_4. A potential of +1.1 V was applied for 10 s followed by a potential of −0.6 V for 24 s. The AuNP surface area was then measured electrochemically. Here, a $Cu/CuSO_4$ reference electrode was used to avoid chloride contamination. A linear sweep was performed from +1.4 V (potential held for 5 s) to 0.5 V at a rate of 0.1 V/s in 0.5 M H_2SO_4. The peak that resulted at approximately +0.8 V was integrated and the surface area determined by using the factor 4 $pC/\mu m^2$ determined by Brummer and Makrides.[22]

Characterization of AuNP Surface. Functionalized electrodes were characterized using SEM. To accomplish this AuNP, functionalized CFME were first backfilled with gallium and grounded to a copper plate using a tungsten wire to limit the effects of charging. A Zeiss Leo Ultra 55 FEG scanning electron microscope was then used to image the tip of each electrode, and nanoparticle size and coverage were determined using the software CellProfiler.[23]

DOI: 10.1021/cn5002667
ACS Chem. Neurosci. 2015, 6, 181−188

Enzyme Labeling. AChE and ChO were resuspended in 5 mM sodium bicarbonate (pH 8.3) at a 2 mg/mL concentration for labeling. AChE and ChO were labeled with Alexa Fluor 488 and Alexa Fluor 555, respectively, according to the protocol provided by Invitrogen.

Immobilization of Enzymes. The tip of each electrode was immersed in a solution containing 0.02 mg/mL AChE and 0.2 mg/mL ChO in 50 mM sodium phosphate buffer, pH 7.4 for 90 min at room temperature. After immersion, the tip of each electrode was washed with deionized water and stored in a solution of 50 mM sodium phosphate buffer at 4 °C.

Quantification of Immobilized Enzymes. The amount of each enzyme present on the AuNP surface was determined following a previously published method for the direct comparison of enzyme to nanoparticle concentrations.[24,25] Briefly, after washing away excess enzyme, the tip of the functionalized CFME was immersed in 20 mM KCN in PBS overnight to dissolve the AuNP surface. A Horiba Jobin Yvon Fluorolog fluorimeter was then used to determine the concentration of each fluorescently labeled enzyme in solution. Enzyme surface coverage was calculating by dividing the amount of enzyme found per electrode by the electrochemically available surface area of the electrode.

Enzyme Kinetics. All measurements were made with 25 mM ACh or choline (unless otherwise noted) in pH 7.4 PBS at room temperature. For this study, activity was defined as micromoles of product detected electrochemically per unit area (to account for the electrode-to-electrode surface area variation and influence of mass transfer on the kinetics). Specific activity was defined as the total activity per milligram of enzyme as determined by the quantification of the immobilized enzymes. The detection rate is defined as the total turnover rate of the electrode.

Flow Cell Experiments. Detection of acetylcholine and choline was tested using a home-built flow cell. The electrode was held at a given potential against a Ag/AgCl reference electrode while a syringe pump was used to flow partially dedeoxygenated solution past the electrode at a rate of 0.25 mL/min. The O_2 concentration in solution was deliberately kept low, as O_2 is a potential interferent, but also an essential cosubstrate for the reaction at the same time. Reference solutions were introduced using a HPLC loop. All data was collected using a CHI or Dagan potentiostat collecting data at a rate of 10 Hz.

Artificial Cell Experiments. Artificial exocytosis measurements were carried out using a surface-immobilized unilamellar liposome model. Briefly, soybean polar lipid extract was dissolved in chloroform and subsequently underwent a dehydration−rehydration method described by Cans et al. to form giant unilamellar liposomes.[26] A single lipid nanotube was formed by using an electrified small glass micropipet to reach the internal leaf of the lipid bilayer. Adhesion of the lipid to the glass tip caused a lipid nanotube to be pulled into the interior of the giant liposome as the micropipet was withdrawn from the liposome surface to the center of the liposome. By microinjection of fluid from the glass pipet into the lipid nanotube, a vesicle was inflated with acetylcholine (10−25 mM) or dopamine (100 μM) to form an artificial secretory vesicle.[26] The ACh biosensor was placed at the lipid nanotube opening and in close contact with the membrane of the cell model for exocytosis, and the release of individual vesicular content of ACh solution was detected by the recordings of amperometric reduction current of H_2O_2 product formation by holding the biosensor at −0.4 V against a Ag/AgCl reference electrode. Vesicular dopamine release from the cell model was detected at the biosensor surface by recordings of the dopamine oxidation current at +0.8 V held against the Ag/AgCl reference electrode. The experimental setup did not allow for degassed solutions to be used during these experiments.

■ ASSOCIATED CONTENT

Supporting Information

Sensor test for the response of H_2O_2 on bare carbon microelectrode surface compared to gold nanoparticle coated surface (Figure S1); response to choline and acetylcholine and the interference of H_2O_2 at gold nanoparticle coated electrodes characterized for electrodes coated with ChO, AChE or with ChO together with AChE (Figure S2). This material is available free of charge via the Internet at http://pubs.acs.org.

■ AUTHOR INFORMATION

Corresponding Author

*E-mail: cans@chalmers.se.

Author Contributions

A.-S.C. is responsible for the concept. A.-S.C., J.D.K., and M.E.K. designed the sensor. J.D.K. and J.W. constructed and characterized the sensor. Artificial exocytosis data was collected by M.E.K. and analyzed by M.E.K. and J.D.K. SEM images were collected by J.W. and J.D.K.. Sensor response time was characterized by J.W., J.B., and Y.W.. The manuscript was drafted by J.D.K. and A.-S.C., with contributions from M.E.K. and J.W. All authors have given approval to the final version of the manuscript.

Funding

This work has been funded by The Swedish Research Council.

Notes

The authors declare no competing financial interest.

■ ABBREVIATIONS

AChE, acetylcholinesterase; ChO, choline oxidase; AuNP, gold nanoparticles; CFME, carbon fiber microelectrode; SEM, scanning electron microscopy

■ REFERENCES

(1) Hasselmo, M. E. (2006) The Role of Acetylcholine in Learning and Memory. *Curr. Opin. Neurobiol. 16*, 710−715.

(2) Miwa, J. M., Freedman, R., and Lester, H. A. (2011) Neural Systems Governed by Nicotinic Acetylcholine Receptors: Emerging Hypotheses. *Neuron 70*, 20−33.

(3) Charney, D., Coyle, J. T., and Nemeroff, C. (2002) *Neuropsychopharmacology: The Fifth Generation of Progress*, Chapter 1, pages 3−14, American College of Neuropsychopharmacology, Brentwood, TN.

(4) Semba, K., and Fibiger, H. C. (1989) Organization of central cholinergic systems. *Prog. Brain Res. 79*, 37−63.

(5) Day, J. C., Kornecook, T. J., and Quirion, R. (2001) Application of in Vivo Microdialysis to the Study of Cholinergic Systems. *Methods 23*, 21−39.

(6) Kozak, R., Bruno, J. P., and Sarter, M. (2006) Augmented Prefrontal Acetylcholine Release during Challenged Attentional Performance. *Cereb Cortex. 16*, 9−17.

(7) Song, P., Hershey, N. D., Mabrouk, O. S., Slaney, T. R., and Kennedy, R. T. (2012) Mass Spectrometry "Sensor" for *in Vivo* Acetylcholine Monitoring. *Anal. Chem. 84*, 4659−64.

(8) Westerink, B. H. C., and De Vries, J. B. (2001) A Method to Evaluate the Diffusion Rate of Drugs from a Microdialysis Probe through Brain Tissue. *J. Neurosci. Methods 109*, 53−58.

(9) Peters, J. L., and Michael, A. C. (1998) Modelling Voltammetry and Microdialysis of Striatal Extracellular Dopamine: The impact of Dopamine Uptake on Extraction and Recovery Ratios. *J. Neurochem. 70*, 594−603.

(10) Bruno, J. P., Gash, C., Martin, B., Zmarowski, A., Pomerleau, P., Burmeister, J., Huett, P., and Gerhardt, G. A. (2006) Second-by-second Measurement of Acetylcholine Release in Prefrontal Cortex. *Eur. J. Neurosci. 24*, 2749−2757.

(11) Hochstetler, S. E., and Wightman, R. M. (1998) Detection of Secretion by Electrochemical Methods. In *On-Line Biophysics Textbook* (Bloomfield, V., and L. De Felice, Eds.), Biophysical Society, Bethesda, MD.

(12) Bruno, J. P., Sarter, M., Gash, C., and Parikh, V. (2006) Choline- and Acetylcholine-Sensitive Microelectrodes. *Encycl. Sens.*, 1−15.

DOI: 10.1021/cn5002667
ACS Chem. Neurosci. 2015, 6, 181−188

(13) Mosharov, E. M., and Sulzer, D. (2005) Analysis of Exocytotic Events Recorded by Amperometry. *Nat. Methods 2*, 651−658.
(14) Amatore, C., Arbault, S., Bonifas, I., and Guille, M. (2009) Quantitative Investigations of Amperometric Spike Feet Suggest Different Controlling Factors of the Fusion Pore in Exocytosis at Chromaffin Cells. *Biophys Chem. 143*, 124−31.
(15) Wilson, G. S., and Gifford, R. (2005) Biosensors for real-time in vivo Measurements. *Biosens. Bioelectron. 20*, 2388−2403.
(16) Hascup, K. N., Hascup, E. R., Pomerleau, F., Huettl, P., and Gerhardt, G. A. (2008) Second-by-Second Measures of L-Glutamate in the Prefrontal Cortex and Striatum of Freely Moving Mice. *J. Pharm. Exp. Ther. 324*, 725−31.
(17) Parikh, V., Pomerleau, F., Huettl, P., Gerhardt, G. A., Sarter, M., and Bruno, J. P. (2004) Rapid Assessment of in vivo Cholinergic Transmission by Amperometric Detection of Changes in Extracellular Choline Levels. *Eur. J. Neurosci. 20*, 1545−54.
(18) Gagner, J. E., Lopez, M. D., Dordick, J. S., and Siegel, R. W. (2011) Effect of Gold Nanoparticle Morphology on Adsorbed Protein Structure and Function. *Biomaterials 32*, 7241−7252.
(19) Keighron, J. D., Åkesson, S., and Cans, A.-S. (2014) Co-immobilization of Acetylcholinesterase and Choline oxidase on Gold Nanoparticles: Stoichiometry, Activity, and Reaction Efficiency. *Langmuir 30*, 11348−55.
(20) Meng, F., Yan, X., Liu, J., Gu, J., and Zou, Z. (2011) Nanoporous Gold as Non-enzymatic Sensor for Hydrogen Peroxide. *Electrochim. Acta 56*, 4657−62.
(21) Finot, M. O., Braybrook, G. D., and McDermott, M. T. (1999) *J. Electroanal. Chem. 466*, 234−241.
(22) Brummer, S. B., and Makrides, A. C. (1964) *J. Electrochem. Soc. 111*, 1122−1128.
(23) Kamentsky, L., Jones, T. R., Fraser, A., Bray, M., Logan, D., Madden, K., Ljosa, V., Rueden, C., Harris, G. B., Eliceiri, K., and Carpenter, A. E. (2011) Improved structure, function, and compatibility for CellProfiler: Modular high-throughput image analysis software. *Bioinformatics 27*, 1179−1180.
(24) Cans, A.-S., Dean, S. L., Reyes, F. E., and Keating, C. D. (2007) Synthesis and Characterization of Enzyme-Au Bioconjugates: HRP and Fluorescein-labeled HRP. *Nanobiotechnology 3*, 12−22.
(25) Keighron, J. D., and Keating, C. D. (2010) Enzyme:Nanoparticle Bioconjugates with Two Sequential Enzymes: Stoichiometry and Activity of Malate Dehydrogenase and Citrate Synthase on Au Nanoparticles. *Langmuir 26*, 18992−19000.
(26) Cans, A.-S., Wittenberg, N., Karlsson, R., Sombers, L., Karlsson, M., Orwar, O., and Ewing, A. G. (2003) Artificial cells: Unique insights into exocytosis using liposomes and lipid nanotubes. *Proc. Natl. Acad. Sci. U. S. A. 100*, 400−404.
(27) Vertegal, A. A., Siegel, R. W., and Dordick, J. S. (2004) Silica Nanoparticle Size Influences the Structure and Enzymatic Activity of Adsorbed Lysozyme. *Langmuir 20*, 6800−6807.
(28) Berg, J. M., Tymoczko, J. L., and Stryer, L. (2007) *Biochemistry*, 6th ed., W. H. Freeman and Company, New York.
(29) Hou, S., Ou, Z., Chen, Q., and Wu, B. (2012) Amperometric acetylcholine biosensor based on self-assembly of gold nanoparticles and Acetylcholinesterase on the sol-gel/multi-walled carbon nantoubes/choline oxidase composite-modified platinum electrode. *Biosens. Bioelectron. 33*, 44−49.
(30) Shi, H., Zhao, Z., Song, Z., Huang, J., Yang, Y., Anzai, J., Osa, T., and Chen, Q. (2005) Fabricating of Acetylcholine Biosensor by a Layer-by-layer Deposition Technique for Determining Trichlorfon. *Electroanalysis 17*, 1285−1290.
(31) Kahn, A., Khan, A. A. P., Asiri, A. M., Rub, M. A., Z, N., Rahman, M. M., Khan, S. B., and Ghani, S. A. (2013) A New Trend on Biosensor for Neurotransmitter Choline/Acetylcholine—An Overview. *Appl. Biochem. Biotechnol. 169*, 1927−1939.
(32) Wang, Z., Zhao, J., Li, F., Gao, D., and Xing, B. (2009) Adsorption and Inhibition of Acetylcholinestease by Different Nanoparticles. *Chemosphere 77*, 67−73.
(33) Izquierdo, D. F., Barbosa, O., Burguite, M. I., Lozano, P., Luis, S. V., Fernandez-Lafuente, R., and Garcia-Verdugo, E. (2014) Tuning lipase B from *Candida antarctica* C-C bond promiscuous activity by immobilization on poly-styrenedivinylbenzene beads. *RSC Adv. 4*, 6219−6225.
(34) Kanik, F. E., Kolb, M., Timur, S., Bahadir, M., and Toppare, L. (2013) An amperometric acetylcholine biosensor based on a conducting polymer. *Int. J. Biol. Macromol. 59*, 111−118.
(35) Xu, Z., Yao, S., Wei, Y., Zhou, J., Zhang, L., Wang, C., and Guo, Y. (2008) Monitoring Enzyme Reaction and Screening of Inhibitors of Acetylcholinesterase by Quantitative Matrix-Assisted Laser Desportion/Ionization Fourier Transform Mass Spectrometry. *J. Am. Soc. Mass. Spectrom. 19*, 1849−1855.
(36) Taylor, P., and Brown, J. H. (1999) Synthesis, Storage, and Release of Acetylcholine. In *Basic Neurochemistry: Molecular, Cellular and Medical Aspects* (Siegel, G. J., Agranoff, B. W., and Albers, R. W., Eds.), 6th ed., Lippincott-Raven, Philadelphia.

DOI: 10.1021/cn5002667
ACS Chem. Neurosci. 2015, 6, 181−188